

Synthesis, Structure, and Solution Reduction Reactions of Volatile and Thermally Stable Mid to Late First Row Transition Metal Complexes Containing Hydrazonate Ligands

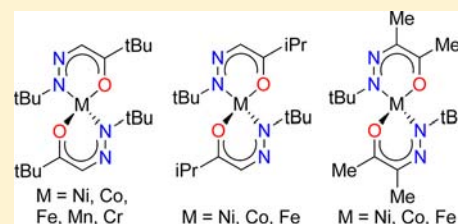
Lakmal C. Kalutarage, Philip D. Martin, Mary Jane Heeg, and Charles H. Winter*

Department of Chemistry, Wayne State University, Detroit, Michigan 48202, United States

Supporting Information

ABSTRACT: Treatment of MCl_2 ($M = Ni, Co, Fe, Mn, Cr$) with 2 equiv of the hydrazonate salts $K(tBuNNCHCtBuO)$, $K(tBuNNCHCiPrO)$, or $K(tBuNNCMeCMeO)$ afforded the complexes $M(tBuNNCHCtBuO)_2$ ($M = Ni, 65\%; Co, 80\%; Fe, 83\%; Mn, 68\%; Cr, 64\%$), $M(tBuNNCHCiPrO)_2$ ($M = Ni, 63\%; Co, 86\%; Fe, 75\%$), and $M(tBuNNCMeCMeO)_2$ ($M = Ni, 34\%; Co, 29\%; Fe, 27\%$). Crystal structure determinations of $Co(tBuNNCHCtBuO)_2$, $M(tBuNNCHCiPrO)_2$ ($M = Ni, Co$), and $M(tBuNNCMeCMeO)_2$ ($M = Ni, Co, Fe$) revealed monomeric complexes with tetrahedral geometries about the metal centers.

To evaluate the potential of these new complexes as film growth precursors, preparative sublimations, thermogravimetric analyses, solid state decomposition studies, and solution reactions with reducing coreagents were carried out. $M(tBuNNCHCtBuO)_2$ sublime between 120 and 135 °C at 0.05 Torr, whereas $M(tBuNNCHCiPrO)_2$ and $M(tBuNNCMeCMeO)_2$ sublime between 100 and 105 °C at the same pressure. All complexes afforded $\geq 96\%$ recovery of sublimed material, with $\leq 3\%$ of nonvolatile residues. The solid state decomposition temperatures were highest for $M(tBuNNCHCiPrO)_2$ (273–308 °C), intermediate for $M(tBuNNCHCtBuO)_2$ (241–278 °C), and lowest for $M(tBuNNCMeCMeO)_2$ (235–250 °C). Treatment of $Co(tBuNNCHCtBuO)_2$ in tetrahydrofuran with hydrazine, $BH_3(L)$ ($L = NHMe_2, SMe_2, THF$), pinacol borane, and $LiAlH_4$ led to rapid formation of cobalt metal, while analogous reductions of $Mn(tBuNNCHCtBuO)_2$ with $BH_3(THF)$, pinacol borane, and $LiAlH_4$ appeared to afford manganese metal. The new complexes $M(tBuNNCHCtBuO)_2$, $M(tBuNNCHCiPrO)_2$, and $M(tBuNNCMeCMeO)_2$ have very promising properties for use as precursors for the growth of the respective metals in atomic layer deposition film growth processes.



INTRODUCTION

Metallic thin films of the first row transition metal elements copper, nickel, cobalt, iron, manganese, and chromium have many important current and future applications. These include copper interconnects in microelectronics devices,^{1–3} chromium, cobalt, and other metal seed layers for copper metallization,^{1–3} cobalt capping layers for copper lines,⁴ manganese- and chromium-based copper diffusion barriers,^{5–7} magnetic metals such as nickel, cobalt, and iron for magneto-resistive random access memory devices,⁸ catalytic applications,⁹ and cobalt, nickel, cobalt silicide, and nickel silicide for contact materials in microelectronics devices.¹⁰ Many of these applications are required for advanced microelectronics devices.³ The smallest feature sizes are scheduled to be less than 20 nm in 2014, and existing thin film deposition processes will not be able to provide the required thickness control and conformality in high aspect ratio features.^{3,11}

The atomic layer deposition (ALD) technique produces inherently conformal films and affords subnanometer film thickness control because of its self-limited growth mechanism.¹² In an ALD cycle, a metal precursor is transported in the vapor phase into the reaction chamber, where it chemisorbs upon the substrate surface reactive sites. Once all accessible surface sites have reacted with the precursor, the surface is saturated and no further reactions can occur. Unreacted

precursor molecules and reaction products are then removed with an inert gas purge. Next, a second precursor vapor is passed over the substrate, which reacts with surface-bound metal precursors to afford the desired thin film material. Finally, a second inert gas purge is passed through the reactor to remove reaction products and excess second precursor. In a well-behaved ALD process, the growth rate per cycle is constant, and thus the film thickness is dependent only upon the number of deposition cycles. ALD precursors need to be thermally stable at the deposition temperature, or else chemical vapor deposition (CVD)-like growth occurs through precursor decomposition.¹² In addition, the metal precursor should be highly reactive toward the second precursor to afford the desired thin film material.

Transition metal thin films must be grown by ALD to meet the conformality and thickness uniformity requirements in nanotechnology and the microelectronics industry. Ideally, the metals should be deposited at ≤ 150 °C to obtain smooth film surfaces, encourage efficient nucleation, and yield continuous films at all film thicknesses.¹³ Thermal ALD is preferable to plasma ALD, since plasmas can lead to substrate damage and poor conformal coverage in high aspect ratio features.¹⁴ As a

Received: February 7, 2013

Published: April 25, 2013



general guide, ALD precursors for transition metal thin films should be thermally stable at ≥ 200 °C and should sublime at the lowest possible temperatures to permit a broad, low temperature deposition window.

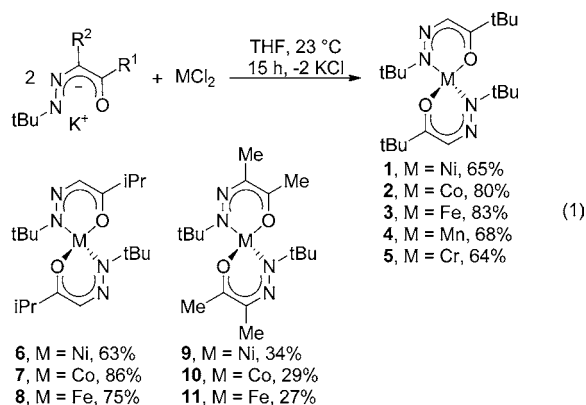
ALD processes and precursors are best developed for copper, and are much less so for nickel, cobalt, iron, manganese, and chromium. Examples of copper ALD processes include $\text{CuL}_2/\text{ZnEt}_2$ at 100–150 °C (L = anionic, bidentate O,N or N,N ligand),^{13,15} $\text{Cu}(\text{thd})_2/\text{H}_2$ at 190–260 °C (thd = 2,2,6,6-tetramethyl-3,5-heptanedionate),¹⁶ $[\text{Cu}(\text{sBuNCMeNsBu})_2]/\text{H}_2$ at 150–250 °C,^{17–19} $\text{Cu}(\text{hfac})_2/\text{isopropanol}$ at 300 °C (hfac = 1,1,1,5,5,5-hexafluoro-2,4-pentanedionate),²⁰ CuCl/H_2 at 360–410 °C,²¹ and CuCl/Zn at 440–500 °C.²² ALD growth was reported from a copper(I) β -diketiminato precursor and diethylsilane,²³ but it was later shown that this process occurs by pulsed CVD and not ALD.²⁴ Related ALD-like routes to copper metal include reduction of CuO films by isopropanol,²⁵ reduction of Cu_3N films with H_2 ,²⁶ and reduction of Cu_2O films on ruthenium seed layers by formic acid.²⁷ Plasma ALD processes have included $\text{Cu}(\text{acac})_2/\text{H}_2$ plasma (acac = 2,4-pentanedionate)²⁸ and $\text{Cu}(\text{OCHMeCH}_2\text{NMe}_2)_2/\text{H}_2$ plasma.²⁹ General problems with copper ALD processes reported to date include unacceptably high growth temperatures, lack of self-limited growth because of precursor thermal decomposition, low reactivity of the copper precursors toward the reducing coreagents, incorporation of zinc with ZnEt_2 , and substrate damage and low conformal coverage in plasma processes. We recently described a copper ALD process that avoids many of the previous problems. The process entails $\text{Cu}(\text{OCHMeCH}_2\text{NMe}_2)_2$, formic acid, and hydrazine,³⁰ which affords self-limited growth between 100 and 170 °C and a growth rate of 0.50 Å/cycle within this temperature range. Reported ALD precursors for nickel films contain amidinate, alkoxide, or cyclopentadienyl ligands, and reducing coreagents have included ammonia plasma, hydrogen plasma, and H_2 .^{10,17} Growth of cobalt films by ALD has employed precursors with cyclopentadienyl, amidinate, and/or carbonyl ligands.^{17,31} The reducing coreagents for cobalt ALD growth were 1,1-dimethylhydrazine, ammonia plasma, hydrogen plasma, nitrogen plasma, and H_2 . The ALD growth of iron metal on aerogels was claimed,³² but details were not reported. The thermal ALD of manganese and chromium films has not been reported, but the plasma ALD growth of Cu/Mn alloy films was recently described with a manganese β -diketonate precursor.³³ Existing ALD precursors for copper, nickel, and cobalt generally have low thermal stabilities and poor reactivities toward reducing agents at < 200 °C.^{10,17,31–33}

We recently reported the synthesis, structure, and precursor properties of a series of copper, nickel, cobalt, iron, manganese, and chromium complexes containing carbohydrazide ligands of the general formula L^1 (Chart 1).³⁴ Copper(II), nickel(II), cobalt(II), and chromium(II) complexes containing L^1 formed monomeric species, but only the copper, nickel, and cobalt complexes were volatile. Additionally, the iron(II) and

manganese(II) complexes formed nonvolatile, dimeric complexes. The five-membered rings formed upon bidentate coordination of L^1 to the metal ions are not sufficiently bulky to block dimerization of the larger metal ions and may not protect the metal centers from intermolecular decomposition pathways. We reasoned that six-membered chelate rings might provide additional steric protection of the metal centers, and could thus lead to monomeric, volatile, and thermally stable complexes. Herein, we report the synthesis, structure, and precursor properties of a series of monomeric nickel, cobalt, iron, manganese, and chromium complexes that contain the hydrazonate ligands L^2 – L^4 (Chart 1). These complexes have tunable volatilities, high decomposition temperatures, and thus have useful ALD precursor properties. The coordination chemistry of hydrazonate ligands is poorly developed to date, and is limited to a few copper(II) and nickel(II) complexes containing aryl groups on the terminal nitrogen atom.³⁵ There is a small family of crystallographically characterized metal complexes that contain the hydrazonate ligand core within more elaborate chelating ligands.³⁶

RESULTS AND DISCUSSION

Synthetic Aspects. The hydrazonate ligand precursors $L^2\text{H}$ – $L^4\text{H}$ (Chart 1) were synthesized and characterized as described in the Experimental Section upon treatment of *tert*-butyl glyoxal, isopropyl glyoxal, or 2,3-butanedione with *tert*-butyl hydrazine hydrochloride and potassium hydroxide. The potassium salts KL^2 – KL^4 were prepared by treatment of $L^2\text{H}$ – $L^4\text{H}$ with KH in tetrahydrofuran, and these solutions were then treated directly with anhydrous MCl_2 (M = Ni, Co, Fe, Mn, Cr,) as depicted in eq 1 to afford complexes **1**–**11** as crystalline



solids in the indicated yields upon sublimation between 100 and 135 °C at 0.05 Torr. Similar treatment of MnCl_2 and CrCl_2 with KL^3 afforded products in very low yields, and isolable products were not obtained upon treatment of these chlorides with KL^4 . Treatment of CuCl_2 with KL^2 – KL^4 resulted in the precipitation of copper metal and use of LiL^2 – LiL^4 did not afford isolable products.

The structures of **1**–**11** were assigned by spectral and analytical data. In addition, X-ray crystal structure of **2**, **6**, **7**, and **9**–**11** were determined, as described below. Complexes **1**–**11** are paramagnetic and show very broad peaks in their ^1H NMR spectra. The magnetic moment values of **1**–**11** are consistent with high spin tetrahedral geometries. Additionally, the solid state and solution state magnetic moment values of **1**–**11** were close to each other, suggesting similar monomeric, tetrahedral structures in the solid state and solution.

Chart 1. Chemical Structures of L^1 – L^4

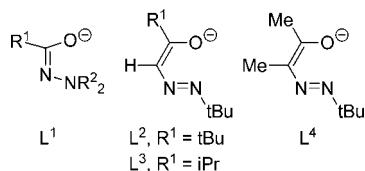


Table 1. Experimental Crystallographic Data for **2**, **6**, **7**, and **9–11**

	2	6	7	9	10	11
empirical formula	C ₂₀ H ₃₈ CoN ₄ O ₂	C ₁₈ H ₃₄ NiN ₄ O ₂	C ₁₈ H ₃₄ CoN ₄ O ₂	C ₁₆ H ₃₀ NiN ₄ O ₂	C ₁₆ H ₃₀ CoN ₄ O ₂	C ₁₆ H ₃₀ FeN ₄ O ₂
fw	425.48	397.19	397.43	369.14	369.38	366.38
space group	<i>P</i> 2 ₁ 2 ₁ 2 ₁	<i>Pbca</i>	<i>Pbca</i>	<i>P</i> 2 ₁ 2 ₁ 2	<i>P</i> 2 ₁ 2 ₁ 2	<i>P</i> 12 ₁ 1
<i>a</i> (Å)	11.0676(8)	10.7214(6)	10.799(2)	31.3403(7)	31.287(2)	11.2423(9)
<i>b</i> (Å)	11.0757(7)	11.3118(6)	11.334(2)	8.0896(2)	8.1317(6)	8.1136(7)
<i>c</i> (Å)	18.946(1)	34.753(2)	34.616(5)	11.1323(3)	11.1558(8)	31.476(3)
<i>V</i> (Å ³)	2322.4(3)	4214.7(4)	4237(1)	2822.4(1)	2838.2(4)	2871.1(4)
<i>Z</i>	8	8	8	4	6	2
<i>T</i> (K)	100(2)	100(2)	100(2)	100(2)	100(2)	100(2)
λ (Å)	0.71073	0.71073	0.71073	0.71073	0.71073	0.71073
density calcd (g cm ⁻³)	1.214	1.271	1.240	1.317	1.297	1.280
μ (mm ⁻¹)	0.759	0.940	0.827	1.046	0.921	0.802
R(<i>F</i>) ^a (%)	3.86	3.27	3.72	2.44	2.98	7.92
Rw(<i>F</i>) ^b (%)	13.35	14.46	13.27	7.04	6.87	27.92

$${}^a R(F) = \frac{\sum ||F_o| - |F_c||}{\sum |F_o|}, \quad {}^b R_w(F^2) = \left[\frac{\sum w(F_o^2 - F_c^2)^2}{\sum w(F_o^2)^2} \right]^{1/2}.$$

Table 2. Selected Bond Lengths (Å) and Angles (deg) for **2**, **6**, **7**, and **9–11**

	2	6	7	9^a	10^a	11^b
M–O	1.910(1)	1.9067(9)	1.920(1)	1.903(1)	1.921(1)	1.919(5)
	1.911(1)	1.904(1)	1.919(1)	1.904(1)	1.921(1)	1.914(5)
M–N	1.963(2)	1.943(1)	1.956(2)	1.925(1)	1.945(2)	2.002(5)
	1.962(2)	1.941(1)	1.956(2)	1.931(1)	1.949(2)	1.982(5)
				1.926(1)	1.944(2)	
C–O	1.283(3)	1.280(2)	1.281(2)	1.275(2)	1.279(2)	1.262(8)
	1.282(3)	1.280(2)	1.286(2)	1.278(2)	1.276(2)	1.279(9)
N–N	1.286(3)	1.280(2)	1.288(2)	1.290(2)	1.296(2)	1.309(7)
	1.287(3)	1.279(1)	1.291(2)	1.289(2)	1.287(2)	1.302(7)
C–C _{core}	1.399(4)	1.383(2)	1.387(3)	1.402(2)	1.405(3)	1.40(1)
	1.380(4)	1.387(2)	1.383(3)	1.405(2)	1.405(3)	1.39(1)
C–N _{core}	1.337(3)	1.350(2)	1.352(2)	1.348(2)	1.351(3)	1.354(9)
	1.361(3)	1.352(2)	1.363(3)	1.347(2)	1.358(2)	1.343(9)
N–M–O	95.12(7)	93.58(4)	95.23(6)	91.96(5)	93.91(6)	91.0(2)
	95.13(7)	93.23(4)	96.01(6)	91.76(5)	93.83(6)	91.6(2)
	115.62(7)	114.42(4)	116.03(6)	91.64(5)	94.37(6)	120.6(2)
	115.43(7)	118.10(4)	113.64(6)	116.72(5)	113.22(6)	116.8(2)
				119.43(5)	117.81(6)	
N–M–N	122.12(7)	119.08(4)	121.48(6)	113.54(5)	115.58(6)	
				125.07(8)	126.17(7)	120.3(2)
O–M–O	114.99(6)	120.60(4)	115.99(6)	126.35(5)	124.85(9)	
				116.74(8)	113.10(6)	119.2(2)
			116.19(5)	113.43(6)		

^aAsymmetric unit contains 1.5 independent molecules. ^bAsymmetric unit contains 3 independent molecules; only data for molecule with Fe1 are listed.

X-ray Crystal Structures. The X-ray crystal structures of **2**, **6**, **7**, and **9–11** were obtained to establish the solid state configurations. Experimental crystallographic data are summarized in Table 1 and selected bond lengths and angles are presented in Table 2. Representative perspective views of **2**, **7**, and **10** are shown in Figures 1–3. The spectral and analytical data of **1**, **3**, **4**, **5**, and **8** are similar to those of **2**, **6**, **7**, and **9–11**, which suggest that **1**, **3**, **4**, **5**, and **8** also adopt monomeric, tetrahedral structures.

The molecular structures of **2**, **6**, **7**, and **9–11** are remarkably similar. All display distorted tetrahedral geometry about the metal centers with κ^2 -N,O coordination of L²–L⁴ through the carbonyl oxygen atom and terminal nitrogen atom. The metal–oxygen distances fall into the narrow range of 1.903 to 1.921 Å. The metal–nitrogen distances lie between 1.925 and 1.963 Å for **2**, **6**, **7**, **9**, and **10**, but are 1.982(5) and 2.002(5) Å in **11**. The slightly longer iron–nitrogen bond lengths in **11** are consistent with the larger iron(II) ion, compared to the slightly smaller cobalt(II) and nickel(II) ions in **2**, **6**, **7**, **9**, and **10**. The

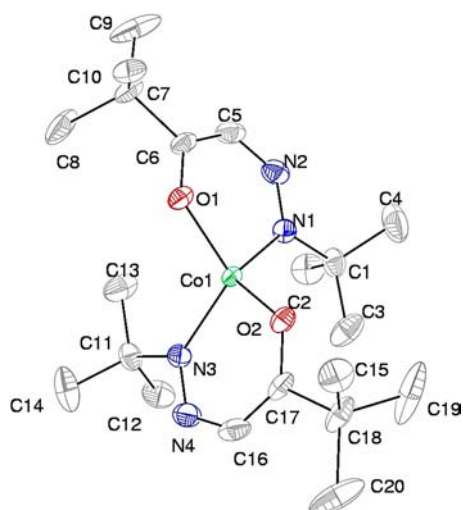


Figure 1. Perspective view of **2** with thermal ellipsoids at the 50% probability level.

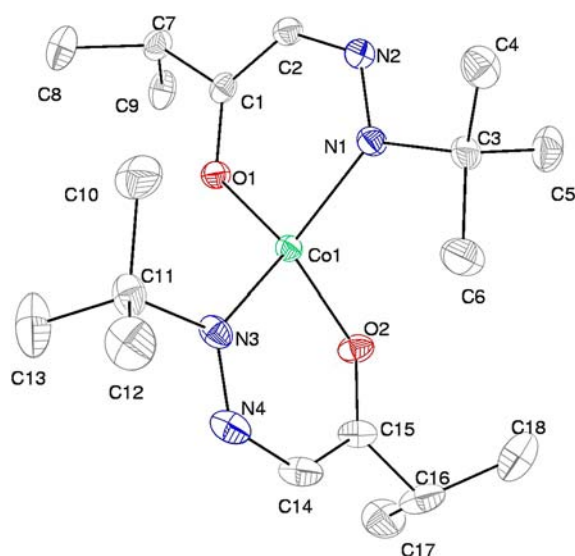


Figure 2. Perspective view of **7** with thermal ellipsoids at the 50% probability level.

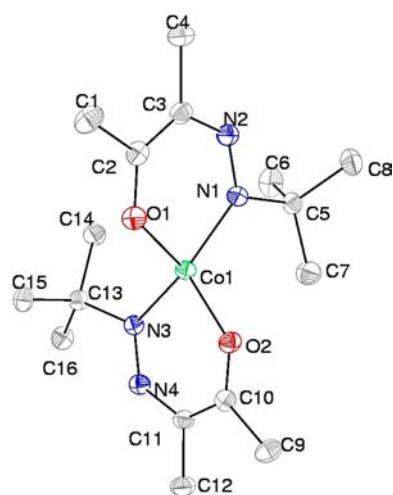


Figure 3. Perspective view of **10** with thermal ellipsoids at the 50% probability level.

nitrogen–nitrogen, carbon–carbon, and carbon–oxygen bond lengths within the L^2-L^4 cores are in between the lengths expected for single and double bonds, which suggest monoanionic, delocalized ligands. The intraligand nitrogen–metal–oxygen angles for **2**, **6**, **7**, and **9–11** fall between 91 and 96° , and the interligand angles range from 113.2 to 120.6° . The corresponding interligand nitrogen–metal–nitrogen and oxygen–metal–oxygen angles are between 119.1 and 126.4° and 113.1 and 120.6° , respectively. These angles illustrate the distorted tetrahedral geometry about the metal ions.

There have been three previously reported crystal structures of copper(II) complexes containing hydrazonate ligands with aryl groups on the terminal nitrogen atom and acyl groups on the central carbon atom of the ligand.³⁵ As noted above, attempts to prepare copper(II) complexes containing L^2-L^4 resulted in the precipitation of copper metal and coordination complexes could not be isolated. The presence of electron-withdrawing phenyl and acyl groups on the ligand cores must render the ligands less basic than L^2-L^4 , thus preventing the reduction of the copper(II) ion. The complex $\text{Ni}(\text{PhNNC}(\text{COMe})\text{C}(\text{Me})\text{O})_2$ is the only other first row transition metal hydrazonate complex that has been crystallographically characterized.^{35b} This complex adopts square planar geometry about nickel, apparently because of the lower steric profile of the ligand compared to the larger L^2-L^4 in **2**, **6**, **7**, and **9–11**. The nickel–nitrogen and nickel–oxygen distances in $\text{Ni}(\text{PhNNC}(\text{COMe})\text{C}(\text{Me})\text{O})_2$ are $1.882(2)$ and $1.816(2)$ Å, respectively, which are shorter than those of **6** and **9** because of the differing geometries. Several similar complexes containing $\kappa^2\text{-N,O-}\beta\text{-ketiminate}$ or related N,O-based ligands with tetrahedral geometries about the metal ions have been structurally characterized, including a nickel(II) pyrazolanoto complex ($\text{Ni}-\text{O}$ $1.924(1)$ Å, $\text{Ni}-\text{N}$ $1.951(1)$ Å),³⁷ a cobalt(II) pyrazolanoto complex ($\text{Co}-\text{O}$ $1.932(2)$, $1.933(2)$ Å, $\text{Co}-\text{N}$ $1.969(2)$, $1.982(2)$ Å),³⁸ and $\text{Fe}(\text{iPrNC}(\text{Me})\text{CHC}(\text{Me})\text{O})_2$ ($\text{Fe}-\text{O}$ $1.9407(8)$, $1.9419(8)$ Å, $\text{Fe}-\text{N}$ $2.0373(9)$, $2.0447(8)$ Å).³⁹ These bond lengths are very similar to those observed in **2**, **6**, **7**, and **9–11**.

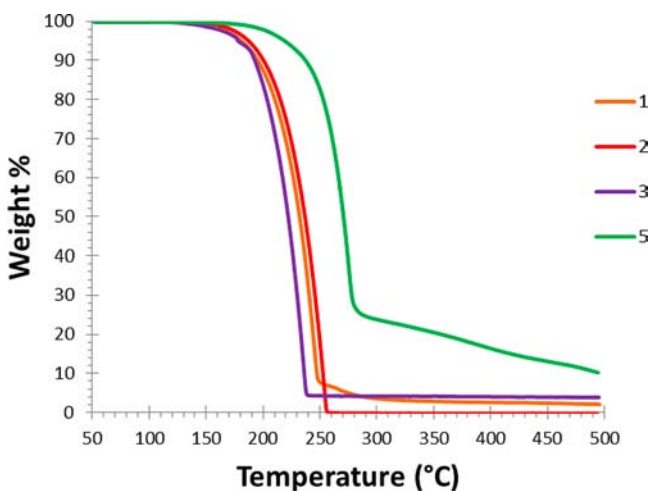
Volatility, Thermal Stability, and Screening of Reducing Co-Reagents. The preparative sublimation data, melting points, and solid state decomposition temperatures for **1–11** are summarized in Table 3. Complexes **1–11** sublime on ~ 0.5 g scales over 3 h between 120 and 135 °C (**1–5**) and 100 – 105 °C (**6–11**) at 0.05 Torr. In all cases, $\geq 96\%$ of the complexes were recovered upon sublimation of analytically pure **1–11**, and $\leq 3\%$ of nonvolatile residues were obtained. The lower sublimation temperatures of **6–11**, compared to **1–5**, are consistent with their lower molecular weights. We have found that preparative sublimation temperatures are approximately the same as those required for precursor delivery in our ALD reactors,³⁰ and thus constitute useful data. Solid state decomposition temperatures were determined as described in the Experimental Section. The decomposition temperatures were highest for **6–8** (273 – 308 °C), intermediate for **1–5** (241 – 278 °C), and lowest for **9–11** (235 – 250 °C). The ligands in **9–11** may not be bulky enough to protect the metal centers from intermolecular decomposition reactions, and the very bulky ligands in **1–5** may lead to decomposition reactions that alleviate steric interactions in the coordination spheres. The thermal decomposition temperature of **6** (273 °C) is much higher than that of the widely promoted nickel(II) film growth precursor $\text{Ni}(\text{iPrNCMeNiPr})$ (180 °C)⁴⁰ and is similar to that of our recently reported complex $\text{Ni}(\text{tBuNNCHCHNtBu})_2$

Table 3. Sublimation Temperature, Melting Point, Solid State Decomposition Temperature, Percent Recovery, and Percent Nonvolatile Residue for 1–11

complex	sublimation temperature (°C/0.05 Torr)	melting point (°C)	solid state decomposition temperature (°C)	% recovery	% nonvolatile residues
1	120	159	245	97	2
2	130	164	260	99	<1
3	120	179	241	99	<1
4	135	171	257	95	2
5	130	276	278	96	3
6	100	94	273	96	<1
7	100	111	308	97	<1
8	105	116	307	97	<1
9	100	135	235	98	1
10	100	145	250	98	2
11	100	122	250	97	2

(290 °C).⁴¹ High thermal stability is very important for ALD precursors, since the precursor thermal decomposition temperature is usually close to the temperature at which loss of self-limited ALD growth occurs and CVD-like growth ensues.^{12,30} Interestingly, **6** melts below its sublimation temperature, and thus vapor transport occurs from the liquid state. Liquid ALD precursors are desirable because they provide more reproducible dosing and may reduce particle levels during film growth.^{12g}

Thermogravimetric analyses (TGA) and differential thermal analysis (DTA) were carried out on **1–11** to understand their thermal stabilities. Representative TGA plots for **1–3** and **5** are shown in Figure 4, and plots for **6–11** are contained in the

**Figure 4.** TGA plots of **1–3** and **5**.

Supporting Information. Complexes **1–3** and **6–11** show similar single step weight losses due to sublimation between 150 and 250 °C in the TGA curves. Complex **4** is very air sensitive and decomposed during the several seconds of ambient atmosphere exposure required to load the TGA balance. Because of its lower volatility, **5** has a single step weight loss between 175 and 290 °C due to sublimation, but also undergoes competitive solid state decomposition at 250–290 °C, leading to a higher nonvolatile residue than the others. Each DTA plot of **1–11** shows two endothermic peaks that are consistent with melting and sublimation. Melting points obtained from DTA curves are similar to the values obtained with a melting point apparatus.

Complexes **2** and **4** were chosen for solution reduction studies, since their electrochemical potentials bracket those of the metal(II) ions in this study (E° (V): Ni, -0.257 ; Co, -0.280 ; Fe, -0.447 ; Mn, -1.185 ; Cr, -0.913).⁴² In these reactions, a solution of **2** or **4** in tetrahydrofuran was treated with a 5-fold molar excess of each potential reducing coreagent listed in Table 4. Reactions that did not afford a black

Table 4. Reactivity of 2 and 4 toward Reducing Agents in Tetrahydrofuran

entry	reducing agent	CoL ₂ (2)	MnL ₂ (4)
1	NH ₂ NH ₂	black powder; ^a sticks to stir bar	no change
2	LiAlH ₄	bubbling, black solution ^a	bubbling, black solution ^a
3	BH ₃ (NHMe ₂)	black solution ^b	no change
4	pinacol borane	black solution ^b	black solution ^b
5	BH ₃ (SMe ₂)	black powder; ^b does not stick to stir bar	became colorless
6	BH ₃ (THF)	black powder; ^a does not stick to stir bar	black solution ^b

^aAmbient temperature. ^bUpon reflux.

precipitate or black solution after 1 h at ambient temperature were then refluxed for 1 h. Treatment of **2** with anhydrous hydrazine at ambient temperature afforded a black precipitate in <0.25 h that stuck to the stir bar, suggesting the formation of magnetic cobalt metal. Indeed, the X-ray powder diffraction spectrum of this powder confirmed crystalline cobalt metal (Supporting Information). Additionally, treatment of **2** with LiAlH₄, BH₃(NHMe₂), pinacol borane, BH₃(SMe₂), or BH₃(THF) either at room temperature (entries 2, 6) or upon reflux (entries 3–5) afforded black powders or black solutions. These black powders did not stick to the magnetic stir bar and showed no reflections in the X-ray diffraction spectra. Annealing of the powder obtained with **2** and BH₃(SMe₂) at 600 °C for 4 h afforded crystalline cobalt metal (Supporting Information). The products of these latter reactions are likely very small cobalt metal nanoparticles. Analogous treatment of **4** with LiAlH₄, pinacol borane, or BH₃(THF) at room temperature (entry 2) or upon reflux (entries 4, 6) afforded black solutions. X-ray diffraction patterns of the reaction products did not show any reflections, even after annealing at 800 °C for 4 h. Manganese metal nanoparticles have been reported from several different synthetic routes, and are oxidized rapidly upon exposure to air.⁴³ While the powders derived from **4** were handled under argon until after annealing

at 800 °C, the argon was not of high purity, and it is possible that there was enough oxygen or water present in the reaction flasks to promote oxidation of small manganese nanoparticles. Treatment of **2** or **4** under the conditions noted above did not yield black precipitates or black solutions with the following reagents: 1,1-dimethylhydrazine, trimethylaluminum, triethylaluminum, triethylsilane, lithium triethylborohydride, $\text{BH}_3(2\text{-picoline})$, $\text{BH}_3(\text{morpholine})$, $\text{B}_{10}\text{H}_{14}$, or 9-borabicyclononane.

Precursor Properties of 1–11. The handful of crystallographically characterized copper and nickel hydrazonate complexes³⁵ contain N-aryl groups and are thus unlikely to be volatile because of π - π stacking interactions in the solid state. Complexes **1–11** combine good volatilities and high thermal stabilities, and **2** and **4** react readily with several hydride coreagents to provide metal powders. These properties suggest that **1–11** may be excellent precursors for use in ALD metal film growth.¹² Importantly, **1–5** contain the same ligand, are all monomeric in the solid state, and **2** and **4** are both reduced by hydride coreagents to the metals. Such similar chemistry should make **1–5** promising precursors for the ALD growth of metal alloy films, such as copper/manganese alloys for self-forming barrier layers,⁵ since ALD growth of metal alloys requires overlap of the self-limited growth temperature ranges for the separate metals.¹² The properties of **1–11** can be compared with several classes of previously reported ALD precursors from our laboratory. The carbohydrazide complexes $\text{M}(\text{Me}_2\text{NNC}(\text{tBu})\text{O})_2$ ($\text{M} = \text{Cu}, \text{Ni}, \text{Co}$) sublime between 70 and 80 °C at 0.05 Torr, and have solid state decomposition temperatures of 255 (Cu), 245 (Co), and 325 °C (Ni).³⁴ These complexes are more volatile than **1–11** and have similar to slightly higher thermal stabilities than **1–11**. However, $\text{Cr}(\text{Me}_2\text{NNCHC}(\text{tBu})\text{O})_2$ is not volatile and the iron(II) and manganese(II) analogues are dimeric and nonvolatile.³⁴ Additionally, $\text{M}(\text{Me}_2\text{NNC}(\text{tBu})\text{O})_2$ have lower reactivities toward reducing coreagents than **2** and **4** to afford metal powders. The 1,2,5-triazapentadienyl complexes $\text{M}(\text{tBuNNCHCHNR})_2$ ($\text{R} = \text{tBu}$ or NMe_2 , $\text{M} = \text{Ni}, \text{Co}, \text{Fe}, \text{Mn}, \text{Cr}$) are monomeric for all metals, sublime at 105 °C ($\text{R} = \text{NMe}_2$) or between 155 and 175 °C ($\text{R} = \text{tBu}$) at 0.05 Torr, and have solid state decomposition points between 280 and 310 °C ($\text{R} = \text{tBu}$) and 181–225 °C ($\text{R} = \text{NMe}_2$).⁴¹ Like **2**, $\text{Ni}(\text{tBuNNCHCHNMe}_2)_2$ is reduced to nickel metal by anhydrous hydrazine in tetrahydrofuran at ambient temperature. Complexes $\text{M}(\text{tBuNNCHCHNtBu})_2$ have higher sublimation temperatures and similar decomposition temperatures, compared to **1–11**, whereas $\text{M}(\text{tBuNNCHCHNMe}_2)_2$ have similar sublimation temperatures to **6–11** but much lower decomposition temperatures. The complexes $\text{M}(\text{tBuNCHCHNtBu})_2$ ($\text{M} = \text{Ni}, \text{Co}, \text{Fe}, \text{Mn}, \text{Cr}$) sublime between 85 and 120 °C/0.05 Torr, have decomposition temperatures between 230 (Ni) and 325 °C (Mn), and decompose thermally to the metals.⁴⁴ The volatilities and thermal stabilities of **1–11** are similar to those of $\text{M}(\text{tBuNCHCHNtBu})_2$, but the thermal decompositions of $\text{M}(\text{tBuNCHCHNtBu})_2$ to the metals are unique because of the self-reduction associated with electron transfer from the radical anionic ligands to the metal.⁴⁴ Few related complexes have been evaluated for their potential to serve as ALD precursors. The β -ketoiminate complexes $\text{M}(\text{iPrNCMeCHCMeO})_2$ ($\text{M} = \text{Cu},$ ^{13a} Fe ³⁹) have been reported. $\text{Cu}(\text{iPrNCMeCHCMeO})_2$ sublimates at 80 °C/0.01 Torr, is reduced to copper metal in solution by diethyl zinc, but appears to decompose thermally at about 200 °C as inferred from the

TGA trace.^{13a} The β -diketiminato complex $\text{Cu}(\text{MeNCMeCHCMeNMe})_2$ sublimates at 80 °C/0.01 Torr with concurrent decomposition.^{13a}

CONCLUSIONS

The hydrazonate complexes **1–11** were prepared by treatment of anhydrous metal(II) chlorides with $\text{K}(\text{tBuNNCHCtBuO})$, $\text{K}(\text{tBuNNCHCtPrO})$, or $\text{K}(\text{tBuNNCMeCMeO})$. Crystal structure determinations of **2**, **6**, **7**, and **9–11** revealed monomeric complexes with tetrahedral geometries about the metal centers, and the similar magnetic moment data in solution and the solid state for **1**, **3**, **5**, **7**, and **8** suggest monomeric, tetrahedral structures. A combination of preparative sublimations, thermogravimetric analyses, solid state decomposition studies, and solution reactions with reducing coreagents suggest that **1–11** are promising precursor for the growth of the respective metals in ALD film growth processes.

EXPERIMENTAL SECTION

General Considerations. All manipulations were carried out under argon using either Schlenk or glovebox techniques, except that the ligands were prepared in ambient atmosphere. Tetrahydrofuran was distilled from sodium benzophenone ketyl, and hexane was distilled from P_2O_5 . Anhydrous transition metal chlorides (CrCl_2 , MnCl_2 , FeCl_2 , CoCl_2 , and NiCl_2) were obtained from Strem Chemicals Inc. and were used as received. $\text{NiCl}_2 \cdot \text{CH}_3\text{CN}$ was prepared according to a literature procedure.⁴⁵ Potassium hydride (30 wt % dispersion in mineral oil; washed with hexane before use) was purchased from Sigma-Aldrich. *tert*-Butyl hydrazine hydrochloride and 3-methylbutanal were purchased from Across Organics. Pinacolone, SeO_2 , and 2,3-butanedione were purchased from Alfa Aesar. 3,3-Dimethyl-2-oxobutanal⁴⁶ and 3-methyl-2-oxobutanal⁴⁷ were prepared using published procedures. The reducing coreagents were obtained from Sigma-Aldrich, Alfa Aesar, or Strem Chemicals Inc. and were used as received.

¹H and ¹³C{¹H} NMR spectra were obtained at 400 and 100 MHz, respectively, in benzene-*d*₆ or chloroform-*d* as indicated and were referenced to the residual proton and carbon resonances of the solvents. Infrared spectra were obtained using Nujol as the medium. Magnetic moments were determined in the solid state using a Johnson Mathey magnetic susceptibility apparatus, and by ¹H NMR in benzene solution using the Evans method.⁴⁸ Melting points were determined on a Thermo Scientific Mel-Temp 3.0 digital melting point apparatus and are uncorrected. TGA and DTA were carried out with a SDT-2960 TGA/DTA instrument.

Preparation of 1-(2-*tert*-Butyl)hydrazono-3,3-dimethylbutan-2-one (L²H). A 100 mL round-bottomed flask was charged with a magnetic stir bar, 3,3-dimethyl-2-oxobutanal (1.00 g, 8.76 mmol), and methanol (15 mL). To this stirred solution at ambient temperature was slowly added a mixture of *tert*-butyl hydrazine hydrochloride (1.114 g, 8.76 mmol) and potassium hydroxide (0.578 g, 8.76 mmol) in methanol (20 mL). This solution was stirred for 6 h. The volatile components were removed under reduced pressure. Light yellow crystals of L²H were obtained upon sublimation of the crude solid at 60 °C/0.05 Torr (1.081 g, 67%): mp 70 °C; ¹H NMR (benzene-*d*₆, 23 °C, δ) 13.01 (s, broad 1H, NH), 7.12 (s, 1H, CHN), 1.11 (s, 9H, C(CH₃)₃), 1.05 (s, 9H, C(CH₃)₃); ¹³C{¹H} NMR (benzene-*d*₆, 23 °C, ppm) 201.22 (s, CO), 119.37 (s, CHN), 54.76 (s, C(CH₃)₃), 41.68 (s, C(CH₃)₃), 28.52 (s, C(CH₃)₃), 27.04 (s, C(CH₃)₃); ESI-MS/MS calcd for C₁₀H₂₁N₂O ([M+H]⁺) 185.1656, found 185.1654.

Preparation of 1-(2-*tert*-Butyl)hydrazono-3-methylbutan-2-one (L³H). A 100 mL round-bottomed flask was charged with a magnetic stir bar, 3-methyl-2-oxobutanal (1.00 g, 9.99 mmol), and methanol (15 mL). To this stirred solution at ambient temperature was slowly added a mixture of *tert*-butyl hydrazine hydrochloride (1.245 g, 9.99 mmol) and potassium hydroxide (0.659 g, 9.99 mmol) in methanol (20 mL). This solution was stirred for 6 h. The volatile components were removed under reduced pressure, and the resultant yellow oily solid

was dissolved in diethyl ether (15 mL). This solution was dried over anhydrous Na_2SO_4 and filtered. The volatile components were then removed under reduced pressure and the resultant yellow oil was vacuum distilled. L^3H was obtained as a yellow liquid that distilled at $48\text{ }^\circ\text{C}/0.05\text{ Torr}$ (0.935 g, 55%): $^1\text{H NMR}$ (CDCl_3 , $23\text{ }^\circ\text{C}$, δ) 6.86 (s, 1H, CHN), 6.63 (s, broad 1H, NH), 3.49 (septet, $J = 7.0\text{ Hz}$, 1H, $\text{CH}(\text{CH}_3)_2$), 1.25 (s, 9H, $\text{C}(\text{CH}_3)_3$), 1.08 (d, 6H, $J = 7.0\text{ Hz}$, $\text{CH}(\text{CH}_3)_2$); $^{13}\text{C}\{^1\text{H}\}$ NMR (CDCl_3 , $23\text{ }^\circ\text{C}$, ppm) 203.69 (s, CO), 131.86 (s, CHN), 54.91 (s, $\text{C}(\text{CH}_3)_3$), 33.98 (s, $\text{CH}(\text{CH}_3)_2$), 28.68 (s, $\text{C}(\text{CH}_3)_3$), 19.00 (s, $\text{CH}(\text{CH}_3)_2$); ESI-HRMS calcd for $\text{C}_9\text{H}_{19}\text{N}_2\text{O}$ ($[\text{M}+\text{H}]^+$) 171.1497, found 171.1497.

Preparation of 3-(2-tert-Butylhydrazono)butan-2-one (L^4H). A 100 mL round-bottomed flask was charged with a magnetic stir bar, 2,3-butanedione (1.000 g, 11.62 mmol), and water (15 mL). To this stirred solution at ambient temperature was slowly added a mixture of *tert*-butyl hydrazine hydrochloride (1.448 g, 11.62 mmol) and potassium hydroxide (0.767 g, 11.62 mmol) in water (20 mL). This solution was allowed to stand for 2 h, during which time the initially formed oil turned to a solid. This solution was filtered, and the solid was dissolved in diethyl ether (10 mL) and allowed to crystallize at $-23\text{ }^\circ\text{C}$ over 24 h. Colorless crystals were obtained by bulb-to-bulb distillation of the crystals obtained from diethyl ether at $60\text{ }^\circ\text{C}/0.05\text{ Torr}$ (0.926 g, 51%): mp $58\text{ }^\circ\text{C}$; $^1\text{H NMR}$ (CDCl_3 , $23\text{ }^\circ\text{C}$, δ) 5.69 (s, broad 1H, NH), 2.28 (s, 3H, $\text{C}(\text{CH}_3)_3$), 1.73 (s, 3H, $\text{C}(\text{CH}_3)_3$), 1.25 (s, 9H, $\text{C}(\text{CH}_3)_3$); $^{13}\text{C}\{^1\text{H}\}$ NMR (CDCl_3 , $23\text{ }^\circ\text{C}$, ppm) 197.16 (s, CO), 139.35 (s, CHN), 54.73 (s, $\text{C}(\text{CH}_3)_3$), 28.82 (s, $\text{C}(\text{CH}_3)_3$), 23.73 (s, $\text{C}(\text{CH}_3)_3$), 6.77 (s, $\text{C}(\text{CH}_3)_3$); ESI-HRMS calcd for $\text{C}_8\text{H}_{17}\text{N}_2\text{O}$ ($[\text{M}+\text{H}]^+$) 157.1342, found 157.1341.

Preparation of Bis(1-tert-butylidiazanyl-3,3-dimethylbut-1-en-2-olate)nickel(II) (1). A 100 mL Schlenk flask was charged with a magnetic stir bar, L^2H (1.000 g, 5.43 mmol), and tetrahydrofuran (30 mL). To this stirred solution at ambient temperature was slowly added KH (0.239 g, 5.97 mmol), and solution was stirred for 4 h. This solution was then slowly added dropwise with a cannula to a stirred suspension of anhydrous $\text{NiCl}_2\cdot\text{CH}_3\text{CN}$ (0.456 g, 2.71 mmol) in tetrahydrofuran (40 mL) at $-78\text{ }^\circ\text{C}$. The resultant dark orange solution was stirred for 15 h at ambient temperature. The volatile components were then removed under reduced pressure, and the resultant dark orange powder was dissolved in hexane (60 mL). The solution was filtered through a 1 cm pad of Celite on a coarse glass frit, and the volatile components were then removed under reduced pressure. Dark orange crystals of **1** (0.749 g, 65%) were obtained by sublimation at $120\text{ }^\circ\text{C}/0.05\text{ Torr}$: mp $157\text{ }^\circ\text{C}$; IR (Nujol, cm^{-1}) 1485 (m), 1362 (m), 1332 (s), 1264 (m), 1246 (m), 1221 (m), 1187 (m), 1116 (m), 1034 (w), 1019 (w), 996 (w), 892 (w), 803 (w); $^1\text{H NMR}$ (benzene- d_6 , $23\text{ }^\circ\text{C}$, δ) 15.35 (s, broad, 2H, $\text{C}(\text{H})\text{N}$), 5.99 (s, 18H, broad, $\text{C}(\text{CH}_3)_3$), -1.24 (s, broad, 18H, $\text{C}(\text{CH}_3)_3$); $\mu_{\text{eff}} = 2.88$ and $2.93\text{ } \mu_{\text{B}}$ in the solid state and in benzene solution, respectively. Anal. Calcd for $\text{C}_{20}\text{H}_{38}\text{NiN}_4\text{O}_2$: C, 56.49; H, 8.88; N, 13.07.

Preparation of Bis(1-tert-butylidiazanyl-3,3-dimethylbut-1-en-2-olate)cobalt(II) (2). In a fashion similar to the preparation of **1**, treatment of anhydrous CoCl_2 (0.350 g, 2.71 mmol) in tetrahydrofuran (40 mL) with a solution of KL^2 (prepared from L^2H (1.000 g, 5.43 mmol) and KH (0.239 g, 5.97 mmol) in tetrahydrofuran (30 mL)) for 15 h at ambient temperature afforded **2** (0.904 g, 80%) as red crystals upon sublimation at $130\text{ }^\circ\text{C}/0.05\text{ Torr}$: mp $162\text{--}164\text{ }^\circ\text{C}$; IR (Nujol, cm^{-1}) 1483 (m), 1462 (s), 1362 (m), 1334 (s), 1264 (m), 1248 (m), 1221 (m), 1189 (m), 1109 (m), 1033 (w), 1018 (w), 995 (w), 894 (w), 805 (m); $\mu_{\text{eff}} = 4.02$ and $3.94\text{ } \mu_{\text{B}}$ in the solid state and in benzene solution, respectively. Anal. Calcd for $\text{C}_{20}\text{H}_{38}\text{CoN}_4\text{O}_2$: C, 56.46; H, 9.00; N, 13.17. Found: C, 56.49; H, 8.86; N, 13.14.

Preparation of Bis(1-tert-butylidiazanyl-3,3-dimethylbut-1-en-2-olate)iron(II) (3). In a fashion similar to the preparation of **1**, treatment of anhydrous FeCl_2 (0.349 g, 2.71 mmol) in tetrahydrofuran (40 mL) with a solution of KL^2 (prepared from L^2H (1.000 g, 5.43 mmol) and KH (0.239 g, 5.97 mmol) in tetrahydrofuran (30 mL)) for 15 h at ambient temperature afforded **3** (0.913 g, 83%) as red crystals upon sublimation at $120\text{ }^\circ\text{C}/0.05\text{ Torr}$: mp $177\text{--}179\text{ }^\circ\text{C}$; IR (Nujol, cm^{-1}) 1492 (m), 1361 (m), 1331 (s), 1264 (m), 1248 (w), 1221 (w), 1187

(m), 1109 (m), 1033 (w), 1019 (w), 991 (w), 892 (w), 822 (w), 808 (w); $\mu_{\text{eff}} = 4.82$ and $4.86\text{ } \mu_{\text{B}}$ in the solid state and in benzene solution, respectively. Anal. Calcd for $\text{C}_{20}\text{H}_{38}\text{FeN}_4\text{O}_2$: C, 56.87; H, 9.07; N, 13.26. Found: C, 56.78; H, 8.98; N, 13.16.

Preparation of Bis(1-tert-butylidiazanyl-3,3-dimethylbut-1-en-2-olate)manganese(II) (4). In a fashion similar to the preparation of **1**, treatment of anhydrous MnCl_2 (0.340 g, 2.71 mmol) in tetrahydrofuran (40 mL) with a solution of KL^2 (prepared from L^2H (1.000 g, 5.43 mmol) and KH (0.239 g, 5.97 mmol) in tetrahydrofuran (30 mL)) for 15 h at ambient temperature afforded **4** (0.774 g, 68%) as dark orange crystals upon sublimation at $135\text{ }^\circ\text{C}/0.05\text{ Torr}$: mp $169\text{--}171\text{ }^\circ\text{C}$; IR (Nujol, cm^{-1}) 1498 (m), 1484 (m), 1363 (m), 1333 (s), 1261 (m), 1220 (w), 1187 (m), 1106 (m), 1090 (w), 1031 (w), 1017 (w), 987 (w), 889 (w), 800 (w); $\mu_{\text{eff}} = 5.73$ and $5.71\text{ } \mu_{\text{B}}$ in the solid state and in benzene solution, respectively. Anal. Calcd for $\text{C}_{20}\text{H}_{38}\text{MnN}_4\text{O}_2$: C, 56.99; H, 9.09; N, 13.29. Found: C, 57.23; H, 9.06; N, 13.36.

Preparation of Bis(1-tert-butylidiazanyl-3,3-dimethylbut-1-en-2-olate)chromium(II) (5). In a fashion similar to the preparation of **1**, treatment of anhydrous CrCl_2 (0.334 g, 2.71 mmol) in tetrahydrofuran (40 mL) with a solution of KL^2 (prepared from L^2H (1.000 g, 5.43 mmol) and KH (0.239 g, 5.97 mmol) in tetrahydrofuran (30 mL)) for 15 h at ambient temperature afforded **5** (0.726 g, 64%) as dark orange crystals upon sublimation at $130\text{ }^\circ\text{C}/0.05\text{ Torr}$: mp $274\text{ }^\circ\text{C}$; IR (Nujol, cm^{-1}) 1507 (m), 1495 (m), 1418 (m), 1364 (s), 1347 (s), 1261 (w), 1219 (w), 1183 (m), 1164 (m), 1115 (m), 1021 (w), 987 (w), 947 (w), 885 (w), 793 (w); $\mu_{\text{eff}} = 2.73$ and $2.91\text{ } \mu_{\text{B}}$ in the solid state and in benzene solution, respectively. Anal. Calcd for $\text{C}_{20}\text{H}_{38}\text{CrN}_4\text{O}_2$: C, 57.39; H, 9.15; N, 13.39. Found: C, 57.54; H, 9.23; N, 13.41.

Preparation of Bis(1-tert-butylidiazanyl-3-methylbut-1-en-2-olate)nickel(II) (6). In a fashion similar to the preparation of **1**, treatment of anhydrous $\text{NiCl}_2\cdot\text{CH}_3\text{CN}$ (0.495 g, 2.93 mmol) in tetrahydrofuran (40 mL) with a solution of KL^3 (prepared from L^3H (1.000 g, 5.87 mmol) and KH (0.259 g, 6.46 mmol) in tetrahydrofuran (30 mL)) for 15 h at ambient temperature afforded **6** (0.724 g, 63%) as dark orange crystals upon sublimation at $100\text{ }^\circ\text{C}/0.05\text{ Torr}$: mp $92\text{--}94\text{ }^\circ\text{C}$; IR (Nujol, cm^{-1}) 1504 (m), 1481 (m), 1363 (s), 1338 (m), 1307 (s), 1262 (m), 1221 (w), 1190 (m), 1120 (m), 1092 (m), 1049 (w), 1022 (w), 999 (w), 802 (m); $^1\text{H NMR}$ (benzene- d_6 , $23\text{ }^\circ\text{C}$, δ) 16.22 (s, broad), 4.74 (s, broad); $\mu_{\text{eff}} = 3.00$ and $3.01\text{ } \mu_{\text{B}}$ in the solid state and in benzene solution, respectively. Anal. Calcd for $\text{C}_{18}\text{H}_{34}\text{NiN}_4\text{O}_2$: C, 54.43; H, 8.63; N, 14.11. Found: C, 54.63; H, 8.55; N, 14.12.

Preparation of Bis(1-tert-butylidiazanyl-3-methylbut-1-en-2-olate)cobalt(II) (7). In a fashion similar to the preparation of **1**, treatment of anhydrous CoCl_2 (0.380 g, 2.93 mmol) in tetrahydrofuran (40 mL) with a solution of KL^3 (prepared from L^3H (1.000 g, 5.87 mmol) and KH (0.259 g, 6.46 mmol) in tetrahydrofuran (30 mL)) for 15 h at ambient temperature afforded **7** (0.989 g, 86%) as red crystals upon sublimation at $100\text{ }^\circ\text{C}/0.05\text{ Torr}$: mp $109\text{--}111\text{ }^\circ\text{C}$; IR (Nujol, cm^{-1}) 1493 (m), 1478 (m), 1364 (m), 1337 (m), 1305 (s), 1264 (w), 1219 (w), 1190 (m), 1113 (m), 1092 (m), 1048 (w), 1021 (w), 998 (w), 913 (w), 865 (w), 807 (m); $\mu_{\text{eff}} = 3.97$ and $3.78\text{ } \mu_{\text{B}}$ in the solid state and in benzene solution, respectively. Anal. Calcd for $\text{C}_{18}\text{H}_{34}\text{CoN}_4\text{O}_2$: C, 54.40; H, 8.62; N, 14.10. Found: C, 54.60; H, 8.74; N, 14.13.

Preparation of Bis(1-tert-butylidiazanyl-3-methylbut-1-en-2-olate)iron(II) (8). In a fashion similar to the preparation of **1**, treatment of anhydrous FeCl_2 (0.371 g, 2.93 mmol) in tetrahydrofuran (40 mL) with a solution of KL^3 (prepared from L^3H (1.000 g, 5.87 mmol) and KH (0.259 g, 6.46 mmol) in tetrahydrofuran (30 mL)) for 15 h at ambient temperature afforded **8** (0.862 g, 75%) as red crystals upon sublimation at $105\text{ }^\circ\text{C}/0.05\text{ Torr}$: mp $114\text{--}116\text{ }^\circ\text{C}$; IR (Nujol, cm^{-1}) 1488 (m), 1359 (s), 1334 (m), 1302 (s), 1262 (m), 1209 (m), 1189 (m), 1114 (m), 1091 (m), 994 (w), 910 (w), 807 (m); $\mu_{\text{eff}} = 5.14$ and $4.73\text{ } \mu_{\text{B}}$ in the solid state and in benzene solution, respectively. Anal. Calcd for $\text{C}_{18}\text{H}_{34}\text{FeN}_4\text{O}_2$: C, 54.82; H, 8.69; N, 14.21. Found: C, 54.92; H, 8.58; N, 14.22.

Preparation of Bis(3-tert-butylidiazanylbut-2-en-2-olate)nickel(II) (9). In a fashion similar to the preparation of **1**, treatment of anhydrous

NiCl₂·CH₃CN (0.543 g, 3.22 mmol) in tetrahydrofuran (40 mL) with a solution of KL⁺ (prepared from L⁴H (1.000 g, 6.44 mmol) and KH (0.284 g, 7.08 mmol) in tetrahydrofuran (30 mL)) for 15 h at ambient temperature afforded **9** (0.394 g, 34%) as dark orange crystals upon sublimation at 100 °C/0.05 Torr: mp 120–122 °C; IR (Nujol, cm⁻¹) 1500 (m), 1405 (s), 1357 (s), 1302 (s), 1263 (s), 1237 (m), 1222 (m), 1185 (s), 1148 (s), 1043 (w), 980 (m), 931 (w), 805 (w), 752 (w); ¹H NMR (benzene-*d*₆, 23 °C, δ) 68.51 (s, 6H, C(CH₃)O), 14.70 (s, 18H, C(CH₃)₃), -34.24 (s, 6H, C(CH₃)N); μ_{eff} = 2.75 and 2.67 μ_B in the solid state and in benzene solution, respectively. Anal. Calcd for C₁₆H₃₀NiN₄O₂: C, 52.06; H, 8.19; N, 15.18. Found: C, 52.20; H, 8.21; N, 15.06.

Preparation of Bis(3-tert-butylidiazanylbut-2-en-2-olate)cobalt(III) (10). In a fashion similar to the preparation of **1**, treatment of anhydrous CoCl₂ (0.418 g, 3.22 mmol) in tetrahydrofuran (40 mL) with a solution of KL⁺ (prepared from L⁴H (1.000 g, 6.44 mmol) and KH (0.284 g, 7.08 mmol) in tetrahydrofuran (30 mL)) for 15 h at ambient temperature afforded **10** (0.336 g, 29%) as red crystals upon sublimation at 100 °C/0.05 Torr: mp 142–145 °C; IR (Nujol, cm⁻¹) 1494 (m), 1401 (m), 1359 (m), 1303 (s), 1262 (m), 1231 (w), 1187 (w), 1148 (m), 981 (m), 801 (w), 751 (w); μ_{eff} = 3.95 and 3.69 μ_B in the solid state and in benzene solution, respectively. Anal. Calcd for C₁₆H₃₀CoN₄O₂: C, 52.03; H, 8.19; N, 15.17. Found: C, 52.14; H, 8.17; N, 15.18.

Preparation of Bis(3-tert-butylidiazanylbut-2-en-2-olate)iron(III) (11). In a fashion similar to the preparation of **1**, treatment of anhydrous FeCl₂ (0.408 g, 3.22 mmol) in tetrahydrofuran (40 mL) with a solution of KL⁺ (prepared from L⁴H (1.000 g, 6.44 mmol) and KH (0.284 g, 7.08 mmol) in tetrahydrofuran (30 mL)) for 15 h at ambient temperature afforded **11** (0.313 g, 27%) as red crystals upon sublimation at 100 °C/0.05 Torr: mp 120–122 °C; IR (Nujol, cm⁻¹) 1401 (m), 1361 (m), 1299 (m), 1261 (w), 1227 (w), 1188 (m), 1147 (w), 983 (w), 800 (w), 750 (w); μ_{eff} = 4.80 and 4.65 μ_B in the solid state and in benzene solution, respectively. Anal. Calcd for C₁₆H₃₀FeN₄O₂: C, 52.47; H, 8.26; N, 15.30. Found: C, 52.39; H, 7.99; N, 15.32.

Sublimation Studies. For the sublimation experiments, 2.5 cm diameter, 30 cm long glass tubes were employed. One end of the tube was sealed, and the other end was equipped with a vacuum adapter with a 24/40 male glass joint. In an argon-filled glovebox, the compound to be sublimed (~0.5 g) was loaded into a 1.0 × 4.0 cm glass tube and this tube was placed at the sealed end of the glass sublimation tube. The sublimation tube was fitted with a 24/40 vacuum adapter, and then was inserted into a horizontal Buchi Kugelrohr oven such that about 15 cm of the tube was situated in the oven. A vacuum of 0.05 Torr was established, and the oven was heated to the indicated temperature. The compounds sublimed to the cool zone just outside of the oven. The percent recovery was obtained by weighing the sublimed product. The percent nonvolatile residue was calculated by weighing the 1.0 × 4.0 cm glass tube at the end of the sublimation. Data are given in the text and in Table 3.

Thermal Decomposition Studies. In an argon-filled drybox, a melting point capillary tube was charged with 1–2 mg of a sample of **1–11**, and the end of the tube was sealed with a small amount of stopcock grease. The capillary tube was then removed from the drybox, and the end was flame-sealed. The capillary tube was transferred to an Electrothermal Model 9200 melting point apparatus, and was then heated at 5 °C/min starting at 25 °C. Samples of **1–11** were visually observed for discoloration or other evidence of decomposition. Data are given in the text and in Table 3.

General Procedure for Solution Reduction Reactions. A 100 mL Schlenk flask was charged with a magnetic stir bar, **2** or **4** (0.100 g), and tetrahydrofuran (10 mL). To each stirred solution at ambient temperature was slowly added a reducing agent (5 equiv) mentioned in Table 4, and solution was stirred for 1 h. Solutions that did not afford black powders or black solutions after 1 h at ambient temperature were refluxed for 1 h. For results, see Table 4 and the text.

X-ray Crystallographic Structure Determinations for 2, 6, 7, and 9–11. Diffraction data were measured on a Bruker X8 APEX-II kappa geometry diffractometer with Mo radiation and a graphite

monochromator. Frames were collected at 100 K with the detector at 40 mm, 0.5° between each frame, and were recorded for 5–10 s. APEX-II⁴⁹ and SHELX⁵⁰ software were used in the collection and refinement of the models. All structures contain neutral molecules without ions or solvent. Complexes **9** and **10** contain 1.5 independent but chemically equivalent molecules in the unit cell, whereas **11** contains 3 independent but chemically equivalent molecules in the unit cell.

■ ASSOCIATED CONTENT

📄 Supporting Information

TGA data for **6–11**, DTA data for **1–11**, X-ray powder diffraction spectra of cobalt metal derived from **2**, and X-ray crystallographic data for **2**, **6**, **7**, and **9–11** in CIF format. This material is available free of charge via the Internet at <http://pubs.acs.org>.

■ AUTHOR INFORMATION

Corresponding Author

*E-mail: chw@chem.wayne.edu.

Notes

The authors declare no competing financial interest.

■ ACKNOWLEDGMENTS

This work was supported by the Semiconductor Research Corporation. We thank Dr. Scott B. Clendenning of Intel Corporation for helpful comments.

■ REFERENCES

- (1) Roule, A.; Amuntencei, M.; Deronzier, E.; Haumesser, P. H.; Da Silva, S.; Avale, X.; Pollet, O.; Baskaran, R.; Passemar, G. *Microelectron. Eng.* **2007**, *84*, 2610–2614.
- (2) (a) Winter, C. H. *Aldrichimica Acta* **2000**, *33*, 3–8. (b) Won, Y. S.; Kim, Y. S.; Anderson, T. J.; Reiffort, L. L.; Ghiviriga, I.; McElwee-White, L. *J. Am. Chem. Soc.* **2006**, *128*, 13781–13788. (c) McElwee-White, L. *Dalton Trans.* **2006**, 5327–5333. (d) Koh, W.; Kumar, D.; Li, W.-M.; Sprey, H.; Raaijmakers, I. *J. Solid State Technol.* **2005**, *48*, 54–58. (e) Sim, H. S.; Kim, S.-I.; Kim, Y. T. *J. Vac. Sci. Technol., B* **2003**, *21*, 1411–1414. (f) Lee, B. H.; Yong, K. *J. Vac. Sci. Technol., B* **2004**, *22*, 2375–2379.
- (3) International Technology Roadmap for Semiconductors; <http://www.itrs.net/>.
- (4) Yang, C.-C.; Li, B.; Shobha, H.; Nguyen, S.; Grill, S.; Ye, W.; AuBuchon, J.; Shek, M.; Edelstein, D. *IEEE Electron Device Lett.* **2012**, *33*, 588–590.
- (5) (a) Haneda, M.; Iijima, J.; Koike, J. *Appl. Phys. Lett.* **2007**, *90*, 252107. (b) Usui, T.; Nasu, H.; Takahashi, S.; Shimizu, N.; Nishikawa, T.; Yoshimaru, M.; Shibata, H.; Wada, M.; Koike, J. *IEEE Trans. Electron Devices* **2006**, *52*, 2492–2499. (c) Koike, J.; Wada, M. *Appl. Phys. Lett.* **2005**, *87*, 041911. (d) Iijima, J.; Fujii, Y.; Neishi, K.; Koike, J. *J. Vac. Sci. Technol. B* **2009**, *27*, 1963–1968. (e) Chung, S.-M.; Koike, J. *J. Vac. Sci. Technol. B* **2009**, *27*, L28–L31. (f) Otsuka, Y.; Koike, J.; Sako, H.; Ishibashi, K.; Kawasaki, N.; Chung, S. M.; Tanaka, I. *Appl. Phys. Lett.* **2010**, *96*, 012101. (g) Chen, G. S.; Chen, S. T.; Lu, Y. L. *Electrochem. Commun.* **2010**, *12*, 1483–1486. (h) Lozano, J. G.; Lozano-Perez, S.; Bogan, J.; Wang, Y. C.; Brennan, B.; Nellist, P. D.; Hughes, G. *Appl. Phys. Lett.* **2011**, *98*, 123112. (i) Casey, P.; Bogan, J.; Brennan, B.; Hughes, G. *Appl. Phys. Lett.* **2011**, *98*, 113508. (j) Au, H.; Lin, Y.; Kim, H.; Beh, E.; Liu, Y.; Gordon, R. G. *J. Electrochem. Soc.* **2010**, *157*, D341–D345. (k) Au, H.; Lin, Y.; Gordon, R. G. *J. Electrochem. Soc.* **2011**, *158*, D248–D253. (l) Dixit, V. K.; Neishi, K.; Akao, N.; Koike, J. *IEEE Trans. Device Mater. Reliab.* **2011**, *11*, 295–302.
- (6) Chu, J. P.; Lin, C. H.; John, V. S. *Appl. Phys. Lett.* **2007**, *91*, 132109.

- (7) Barmak, K.; Cabral, C., Jr.; Rodbell, K. P.; Harper, J. M. E. *J. Vac. Sci. Technol., B* **2006**, *24*, 2485–2498.
- (8) (a) Kang, S. H. *JOM* **2008**, *60*, 28–33. (b) Vaz, C. A. F.; Bland, J. A. C.; Lauhoff, G. *Rep. Prog. Phys.* **2008**, *71*, 056501. (c) Shiratsuchi, Y.; Yamamoto, M.; Bader, S. D. *Prog. Surf. Sci.* **2007**, *82*, 121–160.
- (9) Chen, C.-S.; Lin, J.-H.; Lai, T.-W. *Chem. Commun.* **2008**, 4983–4985.
- (10) (a) Lee, H.-B.-R.; Band, S.-H.; Kim, W.-H.; Gu, G. H.; Lee, Y. K.; Chung, T.-M.; Kim, C. G.; Park, C. G.; Kim, H. *Jpn. J. Appl. Phys.* **2010**, *49*, 05FA11. (b) Lee, H.-B.-R.; Gu, G. H.; Son, J. Y.; Park, C. G.; Kim, H. *Small* **2008**, *4*, 2247–2254. (c) Yang, C.-M.; Yun, S.-W.; Ha, J.-B.; Na, K.-I.; Cho, H.-I.; Lee, H.-B.; Jeong, J.-H.; Kong, S.-H.; Hahm, S.-H.; Lee, J.-H. *Jpn. J. Appl. Phys.* **2007**, *46*, 1981–1983. (d) Do, K.-W.; Yang, C.-M.; Kang, I.-S.; Kim, K.-M.; Back, K.-H.; Cho, H.-I.; Lee, H.-B.; Kong, S.-H.; Hahm, S.-H.; Kwon, D.-H.; Lee, J.-H.; Lee, J. H. *Jpn. J. Appl. Phys.* **2006**, *45*, 2975–2979. (e) Chae, J.; Park, H.-S.; Kang, S.-W. *Electrochem. Solid-State Lett.* **2002**, *5*, C64–C66.
- (11) (a) Kim, H. *Surf. Coat. Technol.* **2006**, *200*, 3104–3111. (b) Kim, H. *J. Vac. Sci. Technol., B* **2003**, *21*, 2231–2261. (c) Merchant, S. M.; Kang, S. H.; Sanganeria, M.; van Schravendijk, B.; Mountsier, T. *JOM-J. Min. Met. Mater. Soc.* **2001**, *52*, 43–48. (d) Wang, S.-Q. *MRS Bull.* **1994**, *19*, 30–40. (e) Roule, A.; Amuntencei, M.; Deronzier, E.; Haumesser, P. H.; Da Silva, S.; Avale, X.; Pollet, O.; Baskaran, R.; Passemar, G. *Microelectron. Eng.* **2007**, *84*, 2610–2614.
- (12) (a) Leskelä, M.; Ritala, M. *Angew. Chem., Int. Ed.* **2003**, *42*, 5548–5554. (b) Leskelä, M.; Ritala, M. *Thin Solid Films* **2002**, *409*, 138–146. (c) Leskelä, M.; Ritala, M. *Nanotechnology* **1999**, *10*, 19–24. (d) Niinistö, L. *Curr. Opin. Solid State Mater. Sci.* **1998**, *3*, 147–152. (e) Ritala, M. *Appl. Surf. Sci.* **1997**, *112*, 223–230. (f) Suntola, T. *Thin Solid Films* **1992**, *216*, 84–89. (g) Putkonen, M.; Niinistö, L. *Top. Organomet. Chem.* **2005**, *9*, 125–145.
- (13) (a) Vidjayacoumar, V.; Emslie, D. J. H.; Clendenning, S. B.; Blackwell, J. M.; Britten, J. F.; Rheingold, A. *Chem. Mater.* **2010**, *22*, 4844–4853. (b) Vidjayacoumar, V.; Emslie, D. J. H.; Blackwell, J. M.; Clendenning, S. B.; Britten, J. F. *Chem. Mater.* **2010**, *22*, 4854–4866.
- (14) Profijt, H. B.; Potts, S. E.; van de Sanden, M. C. M.; Kessels, W. M. M. *J. Vac. Sci. Technol., A* **2011**, *25*, 050801.
- (15) Lee, B. H.; Hwang, J. K.; Nam, J. W.; Lee, S. U.; Kim, J. T.; Koo, S.-M.; Baunemann, A.; Fischer, R. A.; Sung, M. M. *Angew. Chem., Int. Ed.* **2009**, *48*, 4536–4539.
- (16) Hsu, I. J.; McCandless, B. E.; Weiland, C.; Willis, B. G. *J. Vac. Sci. Technol., A* **2009**, *27*, 660–667.
- (17) Lim, B. S.; Rahtu, A.; Gordon, R. G. *Nat. Mater.* **2003**, *2*, 748–754.
- (18) Li, Z.; Rahtu, A.; Gordon, R. G. *J. Electrochem. Soc.* **2006**, *153*, C787–C794.
- (19) Li, Z.; Gordon, R. G.; Farmer, D. B.; Lin, Y.; Vlassak, J. *Electrochem. Solid-State Lett.* **2005**, *8*, G182–G185.
- (20) Solanki, R.; Pathangey, B. *Electrochem. Solid-State Lett.* **2000**, *3*, 479–480.
- (21) Mårtensson, P.; Carlsson, J.-O. *Chem. Vap. Deposition* **1997**, *3*, 45–50.
- (22) Juppo, M.; Ritala, M.; Leskelä, M. *J. Vac. Sci. Technol., A* **1997**, *15*, 2330–2333.
- (23) Park, K.-H.; Bradley, A. Z.; Thompson, J. S.; Marshall, W. J. *Inorg. Chem.* **2006**, *45*, 8480–8482.
- (24) Thompson, J. S.; Zhang, L.; Wyre, J. P.; Brill, D. J.; Lloyd, K. G. *Thin Solid Films* **2009**, *517*, 2845–2850.
- (25) Huo, J.; Solanki, R. *J. Mater. Res.* **2002**, *17*, 2394–2398.
- (26) Li, Z.; Gordon, R. G. *Chem. Vap. Deposition* **2006**, *12*, 435–441.
- (27) Waechter, T.; Ding, S.-F.; Hofmann, L.; Mothes, R.; Xie, Q.; Oswald, S.; Detavernier, C.; Schulz, S. E.; Qu, X.-P.; Lang, H.; Gessner, T. *Microelectron. Eng.* **2011**, *88*, 684–689.
- (28) Niskanen, A.; Rahtu, A.; Sajavaara, T.; Arstila, K.; Ritala, M.; Leskelä, M. *J. Electrochem. Soc.* **2005**, *152*, G25–G28.
- (29) Moon, D.-Y.; Han, D.-S.; Shin, S.-Y.; Park, J.-W.; Kim, B. M.; Kim, J. H. *Thin Solid Films* **2011**, *519*, 3636–3640.
- (30) Knisley, T. J.; Ariyasena, T. C.; Sajavaara, T.; Saly, M. J.; Winter, C. H. *Chem. Mater.* **2011**, *23*, 4417–4419.
- (31) (a) Kwon, J.; Saly, M.; Halls, M. D.; Kanjolia, R. K.; Chabal, Y. J. *Chem. Mater.* **2012**, *24*, 1025–1030. (b) Kim, J.-M.; Lee, H.-B.-R.; Lansalot, C.; Dussarrat, C.; Gatineau, J.; Kim, H. *Jpn. J. Appl. Phys.* **2010**, *49*, 05FA10. (c) Li, Z.; Lee, D. K.; Coulter, M.; Rodriguez, L. N. J.; Gordon, R. G. *Dalton Trans.* **2008**, 2592–2597. (d) Lee, H.-B.-R.; Kim, H. *ECS Trans.* **2008**, *16*, 219–225. (e) Kim, K.; Lee, K.; Han, S.; Park, T.; Lee, Y.; Kim, J.; Yeom, S.; Jeon, H. *Jpn. J. Appl. Phys.* **2007**, *46*, L173–L176. (f) Lee, K.; Kim, K.; Park, T.; Jeon, H.; Lee, Y.; Kim, J.; Yeom, S. *J. Electrochem. Soc.* **2007**, *154*, H899–H903. (g) Kim, K.; Lee, K.; Han, S.; Jeong, W.; Jeon, H. *J. Electrochem. Soc.* **2007**, *154*, H177–H181. (h) Lee, H.-B.-R.; Kim, H. *Electrochem. Solid-State Lett.* **2006**, *9*, G323–G325.
- (32) Kucheyev, S. O.; Biener, J.; Baumann, T. F.; Wang, Y. M.; Hamza, A. V.; Li, Z.; Lee, D. K.; Gordon, R. G. *Langmuir* **2008**, *24*, 943–948.
- (33) Moon, D.-Y.; Han, D.-S.; Park, J.-H.; Shin, S.-Y.; Park, J.-W.; Kim, B. M.; Cho, J. Y. *Thin Solid Films* **2012**, *521*, 146–149.
- (34) Karunarathne, M. C.; Knisley, T. J.; Tunstall, G. S.; Heeg, M. J.; Winter, C. H. *Polyhedron* **2013**, *52*, 820–830.
- (35) (a) MacLeod-Carey, D. A.; Bustos, C.; Schott, E.; Alvarez-Thon, L.; Fuentealba, M. *Acta Crystallogr., Sect. E: Struct. Rep. Online* **2007**, *63*, m670–m672. (b) Marten, J.; Seichter, W.; Weber, E. Z. *Anorg. Allg. Chem.* **2005**, *631*, 869–877. (c) Kuzmina, N. P.; Eliseeva, S. V.; Balashov, A. M.; Trojanov, S. I. *Zh. Neorg. Khim.* **2002**, *47*, 1300–1304.
- (36) (a) Kopylovich, M. N.; Mahmudov, K. T.; da Silva, M. F. C. G.; Figiel, P. J.; Karabach, Y. Y.; Kuznetsov, M. L.; Luzyanin, K. V.; Pombeiro, A. J. L. *Inorg. Chem.* **2011**, *50*, 918–931. (b) Kopylovich, M. N.; MacLeod, T. C. O.; Mahmudov, K. T.; da Silva, M. F. C. G.; Pombeiro, A. J. L. *Dalton Trans.* **2011**, *40*, 5352–5361. (c) Kopylovich, M. N.; Nunes, A. C. C.; Mahmudov, K. T.; Haukka, M.; MacLeod, T. C. O.; Martins, L. M. D. R. S.; Kuznetsov, M. L.; Pombeiro, A. J. L. *Dalton Trans.* **2011**, *40*, 2822–2836. (d) Paira, M. K.; Mondal, T. K.; Ojha, D.; Slawin, A. M. Z.; Tiekink, E. R. T.; Samanta, A.; Sinha, C. *Inorg. Chim. Acta* **2011**, *370*, 175–185. (e) Paira, M. K.; Mondal, T. K.; López-Torres, E.; Ribas, J.; Sinha, C. *Polyhedron* **2010**, *29*, 3147–3156. (f) You, W.; Zhu, H.-Y.; Huang, W.; Hu, B.; Fan, Y.; You, X.-Z. *Dalton Trans.* **2010**, *39*, 7876–7880. (g) Mahmudov, K. T.; Kopylovich, M. N.; da Silva, M. F. C. G.; Figiel, P. J.; Karabach, Y. Y.; Pombeiro, A. J. L. *J. Mol. Catal. A: Chem.* **2010**, *318*, 44–50. (h) Emeleus, L. C.; Cupertino, D. C.; Harris, S. G.; Owens, S.; Parsons, S.; Swart, R. M.; Tasker, P. A.; White, D. J. *J. Chem. Soc., Dalton Trans.* **2001**, 1239–1245. (i) Banße, W.; Jager, N.; Ludwing, E.; Schilde, U.; Uhlemann, E.; Lehmann, A.; Mehner, H. Z. *Naturforsch., B: Anorg. Chem., Org. Chem.* **1997**, *52*, 237–242. (j) Moreno, J. M.; Ruiz, J.; Dominguez-Vera, J. M.; Colacio, E.; Galisteo, D.; Kivekäs, R. *Polyhedron* **1994**, *13*, 203–207. (k) Colacio, E.; Dominguez-Vera, J.-M.; Kivekäs, R.; Ruiz, J. *Inorg. Chim. Acta* **1994**, *218*, 109–116. (l) Colacio, E.; Ruiz, J.; Moreno, J. M.; Kivekäs, R.; Sundberg, M. R.; Dominguez-Vera, J. M.; Laurent, J. P. *J. Chem. Soc., Dalton Trans.* **1993**, 157–163. (m) Colacio, E.; Dominguez-Vera, J. M.; Costes, J.-P.; Kivekäs, R.; Laurent, J. P.; Ruiz, J.; Sundberg, M. *Inorg. Chem.* **1992**, *31*, 774–778. (n) Abraham, N.; Capon, J. M.; Nowogrocki, G.; Sueur, S.; Brémard, C. *Acta Crystallogr., Sect. C: Cryst. Struct. Commun.* **1985**, *41*, 706–709. (o) Abraham, N.; Capon, J. M.; Nowogrocki, G.; Sueur, S.; Brémard, C. *Acta Crystallogr., Sect. C: Cryst. Struct. Commun.* **1984**, *40*, 1355–1357.
- (37) Zhang, X.; Zhang, G.-Y.; Chen, D.; Song, Y.-J. *Acta Crystallogr., Sect. E: Struct. Rep. Online* **2008**, *64*, m642.
- (38) Bao, F.; Jiao, Y.-H.; Ng, S. W. *Acta Crystallogr., Sect. E: Struct. Rep. Online* **2006**, *62*, m558–m559.
- (39) Granum, D. M.; Riedel, P. J.; Crawford, J. A.; Mahle, T. K.; Wyss, C. M.; Begej, A. K.; Arulsamy, N.; Pierce, B. S.; Mehn, M. P. *Dalton Trans.* **2011**, *40*, 5881–5890.
- (40) Lim, B. S.; Rahtu, A.; Park, J.-S.; Gordon, R. G. *Inorg. Chem.* **2003**, *42*, 7951–7958.
- (41) Kalutarage, L. C.; Heeg, M. J.; Martin, P. D.; Saly, M. J.; Kuiper, D. S.; Winter, C. H. *Inorg. Chem.* **2013**, *52*, 1182–1184.
- (42) *Handbook of Chemistry and Physics*, 92nd ed.; CRC: Boca Raton, FL, 2011–2012; pp 5–80 to 5–89; <http://www.hbcnpnetbase.com/>.

- (43) (a) Bondi, J. F.; Oyler, K. D.; Ke, X.; Schiffer, P.; Schaak, R. E. *J. Am. Chem. Soc.* **2009**, *131*, 9144–9145. (b) Ward, M. B.; Brydson, R.; Cochrane, R. F. *J. Phys.: Conf. Ser.* **2006**, *26*, 296–299.
- (44) Knisley, T. J.; Saly, M. J.; Heeg, M. J.; Roberts, J. L.; Winter, C. H. *Organometallics* **2011**, *30*, 5010–5017.
- (45) Reedijk, J.; Marshall, W. J. *Recl. Trav. Chim. Pays-Bas* **1968**, *87*, 552–558.
- (46) Fuson, R. C.; Gray, H.; Gouza, J. J. *J. Am. Chem. Soc.* **1939**, *61*, 1937–1940.
- (47) Kwiatowski, P.; Chaładaj, W.; Jurczak, J. *Tetrahedron* **2006**, *62*, 5116–5125.
- (48) Evans, D. F. *J. Chem. Soc.* **1959**, 2003.
- (49) *APEX II collection and processing programs*; Bruker AXS Inc.: Madison WI, 2005.
- (50) Sheldrick, G. M. *Acta Crystallogr.* **2008**, *A64*, 112–122.